Molecular g-values, Magnetic Susceptibility Anisotropies, Molecular Electric Quadrupole Moments, improved Molecular Electric Dipole Moments and ^{14}N-Quadrupole Coupling Constants of Acrylonitrile, $H_2C=CH-CN$, and the Magnetic Susceptibility Tensor of the Nitrile Group

M. Stolze and D. H. Sutter
Abteilung Chemische Physik im Institut für Physikalische Chemie der Universität Kiel

Z. Naturforsch. **40 a**, 998–1010 (1985); received August 12, 1985

The highfield, linear and quadratic Zeeman effect has been observed in Acrylonitrile (Vinyl Cyanide). The Zeeman multiplets are complicated by the presence of the ^{14}N nuclear quadrupole coupling, however the ^{14}N nuclear Zeeman effect effectively uncouples ^{14}N spin from the rotational angular momentum. This uncoupling was used to derive improved molecular electric dipole moments from the Stark-shifts in the $2_{11} \leftarrow 2_{02}$ and $3_{12} \leftarrow 3_{03}$ rotational transitions observed under $\Delta M_J = 0$ selection rule in the presence of a high magnetic field. They are $|\mu_a| = 3.815(12)$D and $|\mu_b| = 0.894(68)$D, respectively. From the zero field hfs multiplets, observed under high resolution conditions, improved ^{14}N quadrupole coupling constants were obtained: $\chi^N_{aa} = -3.7800(21)$ MHZ, $\chi^N_{bb} - \chi^N_{cc} = -0.4200(89)$ MHz. They are discussed with reference to the structure of the Nitrile group. From the Zeeman splittings of the $1_{01} \leftarrow 0_{00}$, $1_{10} \leftarrow 1_{01}$, $2_{11} \leftarrow 2_{02}$ and $3_{12} \leftarrow 3_{03}$ rotational transitions observed under $\Delta M_J = 0$ and $\Delta M_J = \pm 1$ selection rule, the diagonal elements of the molecular g-tensor and the anisotropies in the diagonal elements of the molecular magnetic susceptibility tensor were obtained as $g_{aa} = -0.17901(33)$, $g_{bb} = -0.04585(17)$, $g_{cc} = -0.01820(16)$ and $2\chi_{aa} - \chi_{bb} - \chi_{cc} = -7.22(25)$ 10^{-6} erg G^{-2} mole^{-1} and $2\chi_{bb} - \chi_{cc} - \chi_{aa} = +15.90(31)$ 10^{-6} erg G^{-2} mole^{-1}.

They are discussed with reference to the molecular electric quadrupole moment, the paramagnetic and diamagnetic contributions to the molecular susceptibilities, and the second moments of the electronic charge distribution. The susceptibility data are also used to derive the magnetic susceptibility tensor contribution of the Nitrile group.

Introduction

We started our investigation of the rotational Zeeman effect of Acrylonitrile because of our interest in the changes of the molecular parameters in the isoelectronic series $H_2C=CH-CN$, through $H_2C=N-CN$ to $H_2C=C=C=O$.

Acrylonitrile is a planar asymmetric top molecule whose a-axis (= axis of least principal moment of inertia) forms an angle of approximately 16° with respect to the C–C≡N-bond axis (see Fig. 1). Its vibronic ground state rotational spectrum has been assigned first by Wilcox, Goldstein, and Simmons [1] in 1953. They have also determined the components of the molecular electric dipole moment as $|\mu_a| = 3.68$D and $|\mu_b| = 1.25$D and they have given a first estimate of the aa-component of the ^{14}N nuclear quadrupole coupling constant as $\chi^N_{aa} = -3.0(3)$ MHz. In 1959 Costain and Stoicheff [2] have published their results for six isotopic species from which they have derived a partial r_s-structure (except for the CH_2-group). They have also given improved ^{14}N quadrupole coupling constants i.e. $\chi^N_{aa} = -3.69(5)$ MHz and $\chi^N_{bb} - \chi^N_{cc} = -0.53(19)$ MHz [3]. Extensive centrifugal distortion analyses have been presented in 1973 by Demaison, Bouchy, Roussy, and Barriol [4] and by Gerry and Winnewisser [5]. The first radio astronomical observation has been reported by Gardner and Winnewisser in 1975 [6]. In 1979 the available microwave data have been critically reviewed and tabulated by Gerry, Yamada, and Winnewisser [7].

Reprint requests to Prof. Dr. D. H. Sutter, Abteilung Chemische Physik im Institut für Physikalische Chemie der Universität Kiel, Olshausenstr. 40, D-2300 Kiel, W.-Germany.

0340-4811 / 85 / 1000-0998 $ 01.30/0. – Please order a reprint rather than making your own copy.

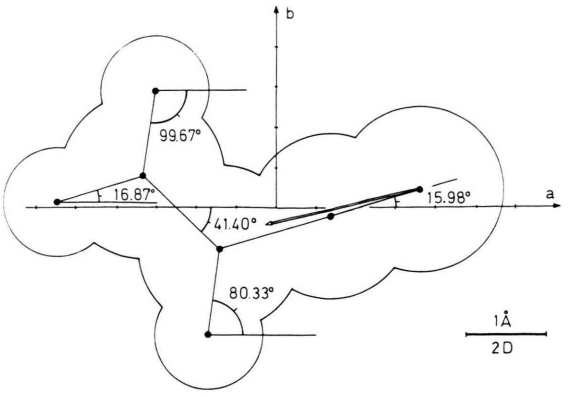

Fig. 1. To scale drawing of the r_s-structure of Acrylonitrile [2] showing the position and orientation of the molecular principal inertia axes system. The angles between the bond axes and the molecular a-axis are given explicitly. They are used later in the derivation of the local susceptibility tensor assigned to the Nitrile group. Also shown is the vector of the molecular electric dipole moment (Table 5). If attached to the position of the ^{14}N nucleus as the most electronegative constituent with its negative end, it points to a position only slightly below the center of gravity of the three protons.

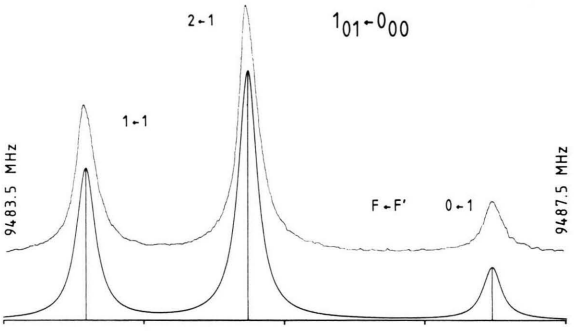

Fig. 2. Zerofield pattern of the $1_{01} \leftarrow 0_{00}$ transition of Acrylonitrile. The underlying simulation is calculated using a Lorentzian line shape with full line width at half height of 150 kHz.

The present rotational Zeeman effect investigation which, from the diagonal elements of the molecular g-tensor and from the anisotropies of the molecular susceptibility tensor, leads to the molecular electric quadrupole moments Q_{aa}, Q_{bb}, Q_{cc} (all referred to the center of mass of the principal inertia axes system; see Fig. 1), further extends our knowledge of the vibronic ground state properties of this molecule. As a byproduct of this high resolution study in oversized waveguide cells improved ^{14}N quadrupole coupling constants and molecular electric dipole moments can be presented, and first values for the elements of the magnetic susceptibility tensor of the Nitrile group can be proposed.

Experimental

Acrylonitrile (99% grade) has been purchased from Aldrich-Chemie and was used after several bulb to bulb destillations without further purification. Unlike $H_2C{=}N{-}C{\equiv}N$ and $H_2C{=}C{=}C{=}O$ the compound proved to be stable in our brass waveguide absorption cells. The standard Stark effect Zeeman spectrometer described earlier [8, 9] with oversized cells (inner cross section 1 cm by 5 cm) and 33 kHz square wave modulation was used for the study of the low J μ_b-type Q-band transitions $1_{10} \leftarrow 1_{01}$ (45334.284 MHz), $2_{11} \leftarrow 2_{02}$ (45795.361 MHz) and $3_{12} \leftarrow 3_{03}$ (46493.486 MHz).

To our knowledge these b-type transitions have never been measured before. Care was taken to minimize standing waves buildup which – in oversized wave guides – may cause dispersion type contributions to the observed line shapes and thus may lead to less reliable frequency determinations. The $1_{01} \leftarrow 0_{00}$ transition (9485.039 MHz) was measured with the superheterodyne bridge spectrometer described recently [10, 11]. The frequencies given above correspond to the hypothetical center frequencies of the observed zerofield ^{14}N hfs patterns [12].

Typical recording conditions were cell temperatures about $-50\,°C$ and sample pressures about 1–2 mTorr. The observed line widths (full half-width at half height) were 150 kHz for the $1_{01} \leftarrow 0_{00}$ transition and about 300 kHz for the other transitions. As an example we present the zero field ^{14}N quadrupole hfs pattern of the $1_{01} \leftarrow 0_{00}$ transition in Figure 2.

Theory and Analysis of the Spectra

First we discuss the zero field spectrum i.e. the ^{14}N quadrupole hfs of the rotational transitions, since the knowledge of the quadrupole coupling constants and of the hypothetical "center frequencies" of the individual quadrupole hyperfine multiplets is a prerequisite for the subsequent analysis of

the rotational Zeeman effect patterns. Second we discuss the high-field rotational Zeeman effect [13]. From the high field Zeeman splittings it is possible to determine the magnetic susceptibility anisotropies and the absolute values of the diagonal elements of the molecular g-tensor but only the relative sign of the g-values is determined from such an experiment.

Third we discuss the intermediate field rotational Zeeman effect. From intermediate field Zeeman patterns (fields about 5 kG in the case of molecules containing ^{14}N nuclei) only less accurate magnetic parameters can be determined, but the correct set of signs for the molecular g-values can be clearly distinguished from the wrong set by comparison of computer simulations of the corresponding predicted spectra with the observed spectrum. Finally we discuss the combined high-field Zeeman-Stark effect observed under $\Delta M_J = 0$ selection rule i.e. with parallel magnetic and electric fields. Since the exterior magnetic field very effectively uncouples nuclear spin and overall rotation via the nuclear Zeeman effect, the analysis of the Stark-shifts of the satellites is easier, both experimentally and theoretically and this leads to a more accurate dipole moment determination.

For the zerofield spectrum we have used the standard rigid rotor Hamiltonian including the quadrupole coupling of the ^{14}N nucleus as given in (1) [14].

$$\hat{H}_{\text{eff}} = \frac{\hbar^2}{2}\left(\frac{1}{I_{aa}}\hat{J}_a^2 + \frac{1}{I_{bb}}\hat{J}_b^2 + \frac{1}{I_{cc}}\hat{J}_c^2\right) + \frac{1}{6}\sum_{\gamma}\sum_{\gamma'} V_{\gamma\gamma'} Q_{\gamma\gamma'}, \tag{1}$$

I_{aa}, I_{bb}, I_{cc} principal moments of inertia.

$\hat{J}_a, \hat{J}_b, \hat{J}_c$ operators corresponding to the components of the rotational angular momentum in direction of the principal inertia axes measured in units of $\hbar$.

$Q_{\gamma\gamma'}$ components of the ^{14}N nuclear quadrupole moment tensor ($\gamma = a, b, c$).

$V_{\gamma\gamma'}$ vibronic ground state expectation values for the second derivatives of the intramolecular Coulomb potential at the position of the ^{14}N nucleus.

Equation (1) represents an effective rotational Hamiltonian. It results from a second order perturbation treatment within the rovibronic states (i.e. a Van Vleck transformation, which aimes at the vibronic ground state). All other spins are neglected. Their coupling to the overall rotation is too weak for detection in the present experiment.

The Hamiltonian matrix corresponding to Eq. (1) was set up in the coupled symmetric top basis $|J, K_a, I, F, M_F\rangle$ and was diagonalized numerically as described previously [15].

The rotational constants and the ^{14}N quadrupole coupling constants were fitted by a least squares procedure to the observed transition frequencies listed in Table 1. They are given in Table 2.

It is interesting to note that our ^{14}N quadrupole coupling constants differ by up to four standard deviations from those presented in [7]. However, the older values resulted from a least squares fit to hfs multiplets measured under considerably less resolution (quoted uncertainties for the single frequencies were on the order of 150 kHz). Since a comparable number of hfs satellites entered into the fit in both cases our results presented in Table 2 are superior and were used for the subsequent analysis of the Zeeman spectra.

In the presence of an exterior magnetic field the effective Hamiltonian (1) has to be supplemented by the effective first and second order molecular Zeeman effect contributions $\hat{H}_{g,\text{eff}}$ and $\hat{H}_{\chi,\text{eff}}$ and by the nuclear Zeeman effect contribution of the quadrupole nucleus $\hat{H}_{NZ}$, here ^{14}N [16]:

$$\hat{H}_{g,\text{eff}} = -\mu_N \frac{H_Z}{2}\sum_{\gamma}\sum_{\gamma'}(\hat{J}_\gamma \cdot g_{\gamma\gamma'}\hat{\Phi}_{\gamma' Z} + \hat{\Phi}_{\gamma Z} g_{\gamma\gamma'}\hat{J}_{\gamma'}), \tag{2}$$

$$\hat{H}_{\chi,\text{eff}} = -\tfrac{1}{2} H_Z^2 \sum_{\gamma}\sum_{\gamma'} \hat{\Phi}_{\gamma Z} \cdot \chi_{\gamma\gamma'} \cdot \hat{\Phi}_{\gamma' Z}, \tag{3}$$

$$\hat{H}_{NZ} = -\mu_N \cdot g_I \cdot H_Z \cdot \hat{I}_Z. \tag{4}$$

$\mu_N = \dfrac{e\hbar}{2m_p c}$ nuclear magneton,

H_Z exterior magnetic field assumed to be directed along the space fixed Z-axis,

$\Phi_{\gamma Z}$ direction cosine between the space fixed Z-axis and the molecular principal inertia axis ($\gamma = a$, b, or c),

$g_{\gamma\gamma}$ element of the effective molecular g tensor,

$$g_{aa} = \frac{m_p}{I_{aa}}\left(\sum_{\nu}^{\text{nuclei}} Z_\nu(b_\nu^2 + c_\nu^2) + \frac{2}{m}\left(\frac{L_a L_a}{\Delta}\right)\right)$$

(and cyclic permutations)

Table 1. Observed frequencies of some ^{14}N-quadrupole hyperfine transitions of Acrylonitrile, and observed and calculated splittings between ^{14}N-quadrupole satellites used for fitting the nuclear quadrupole coupling constants (see Table 2). Also given are the hypothetical rigid rotor center frequencies ν_c, derived from experimental frequencies and calculated hyperfine splittings. The calculated values follow from the final constants given in Table 2 by a numerical diagonalization of the Hamiltonian matrix. The less intense satellites in the $2_{11} \leftarrow 2_{02}$ and $3_{12} \leftarrow 3_{03}$ transitions were not used in the fit. However their calculated frequencies fall within better than ± 10 kHz with the observed values.

$J'\ K'_a\ K'_c \leftarrow J\ K_a\ K_c$	$F' \leftarrow F$	Rel. int.	ν_{exp}/MHz	Splitting between hfs-satellites used to fit the coupling constants	(exp. value)/ MHz	(calcul. value)/ MHz
ν_c/MHz						
1 0 1 ← 0 0 0	1 1	33.3	9 484.093	$\nu_{0\leftarrow1} - \nu_{1\leftarrow1}$	2.839	2.835
	2 1	55.5	9 485.229	$\nu_{0\leftarrow1} - \nu_{2\leftarrow1}$	1.703	1.701
9485.039	0 1	11.1	9 486.932			
1 1 0 ← 1 0 1	1 0	11.1	45 332.920	$\nu_{2\leftarrow2} - \nu_{1\leftarrow0}$	1.073	1.071
	2 2	41.7	45 333.993	$\nu_{1\leftarrow2} - \nu_{1\leftarrow0}$	1.698	1.701
45 334.284	1 2	13.0	45 334.618	$\nu_{2\leftarrow1} - \nu_{1\leftarrow0}$	2.205	2.205
	1 2	13.9	45 335.125	$\nu_{1\leftarrow1} - \nu_{1\leftarrow0}$	2.830	2.835
	1 1	8.3	45 335.750			
2 1 1 ← 2 0 2	2 1	5.0	45 793.988	$\nu_{3\leftarrow3} - \nu_{1\leftarrow1}$	0.376	0.375
	1 1	15.0	45 794.830	$\nu_{2\leftarrow2} - \nu_{3\leftarrow3}$	0.677	0.676
45 795.361	3 3	41.5	45 795.206			
	2 2	23.1	45 795.883			
	3 2	5.2	45 796.434			
	1 2	5.0	45 796.721			
3 1 2 ← 3 0 3	2 2	21.2	46 493.267	$\nu_{3\leftarrow3} - \nu_{4\leftarrow4}$	0.387	0.387
	4 4	40.2	46 493.383			
46 493.486	3 3	28.0	46 493.770			
	4 3	2.7	46 494.660			
	2 3	2.7	46 494.951			

Table 2. Rotational constants and ^{14}N-quadrupole coupling constants $\chi^N_{\gamma\gamma}$ ($\gamma = a, b$ or c) for Acrylonitrile. They are obtained from a least squares fit to the center frequencies and the hyperfine splittings listed in Table 1. The numbers in brackets are the single standard deviations of the fit. They are given in units of the least significant figure.

$A = h/(8\pi^2 I_{aa})$	49848.007(2) MHz
$B = h/(8\pi^2 I_{bb})$	4971.316(1) MHz
$C = h/(8\pi^2 I_{cc})$	4513.722(1) MHz
χ^N_{aa}	−3.7800(21) MHz
$\chi^N_{bb} - \chi^N_{cc}$	−0.4200(89) MHz
χ^N_{bb}	1.6800(46) MHz
χ^N_{cc}	2.1000(46) MHz

[Only the diagonal elements are of relevance here since the off diagonal elements are associated with rotational operators which are off diagonal in the asymmetric top wave functions and thus lead to negligibly small second order contributions to the energy levels].

m_p proton mass,

Z_ν atomic number of ν-th nucleus,

a_ν, b_ν, c_ν coordinates of ν-th nucleus with respect to the molecular principal inertia axes system,

$\hat{L}_a$ a-component of the electronic angular momentum operator,

$$\left(\frac{L_a L_a}{\Delta}\right) = \sum_{n}^{\text{ex. electr. states}} \frac{\langle 0|\hat{L}_a|n\rangle\langle n|\hat{L}_a|0\rangle}{E_0 - E_n}$$

perturbation sum running over the excited electronic states,

$\chi_{\gamma\gamma}$ element of the molecular susceptibility tensor

$$\chi_{aa} = -\frac{e^2}{4mc^2}\left(\langle 0|\sum_{\varepsilon}^{\text{electrons}}(b_\varepsilon^2 + c_\varepsilon^2)|0\rangle + \frac{2}{m}\left(\frac{L_a L_a}{\Delta}\right)\right)$$

(and cyclic permutations)

g_I g-value of the quadrupole nucleus, here $g_I = g_I\,(^{14}\text{N}) = 0.4036)$ [17]. This value includes the average shielding of the nucleus.

Table 3. Observed and calculated frequency-splittings of some Zeeman-hyperfine-satellites of Acrylonitrile with respect to the corresponding hypothetical rigid rotor frequencies (see Table 1). The upper and lower rotational states are designated by the corresponding quantum numbers of the uncoupled representation. For overlapping satellites $\Delta\nu_{\text{calc, av}}$ are intensity averaged values.

Rotational center freq.	Transition magn. field					
$J'\ K'_a\ K'_c \leftarrow J\ K_a\ K_c$ ν_c/MHz	H/kGauß	rel. int.	$M'_J \leftarrow M_J\ M_I$	$\Delta\nu_{\text{exp}}$/MHz	$\Delta\nu_{\text{calc}}$/MHz	$\Delta\nu_{\text{calc, av}}$/MHz
1 0 1 ← 0 0 0		4.	0 0 −1	−0.301	−0.262	−0.289
		4.	0 0 1		−0.338	
9485.039	25.488	4.	0 0 0	0.818	0.819	
1 0 1 ← 0 0 0		2.	−1 0 0	−0.904	−0.907	
		2.	−1 0 −1	−0.351	−0.288	−0.358
9485.039	18.704	2.	−1 0 1		−0.429	
		2.	1 0 0	0.112	0.109	
		2.	1 0 −1	0.711	0.793	0.709
		2.	1 0 1		0.624	
1 1 0 ← 1 0 1		4.	−1 −1 −1	−1.784	−1.829	−1.790
		4.	−1 −1 1		−1.752	
45334.284	24.390	4.	−1 −1 0	−0.910	−0.919	
		4.	1 1 −1	1.176	1.131	1.179
		4.	1 1 1		1.226	
		4.	1 1 0	2.086	2.079	
1 1 0 ← 1 0 1		2.	−1 0 0	−2.087	−2.088	
		2.	−1 0 −1	−1.307	−1.341	−1.308
45334.284	17.510	2.	−1 0 1		−1.276	
		2.	1 0 −1	1.746	1.701	1.735
		2.	1 0 1		1.769	
2 1 1 ← 2 0 2		16.	−2 −2 −1	−1.382	−1.409	−1.381
		16.	−2 −2 1		−1.354	
45795.361	24.895	16.	−2 −2 0	−0.930	−0.929	
		4.	−1 −1 −1	−0.486	−0.520	−0.486
		4.	−1 −1 1		−0.453	
		4.	1 1 0	0.513	0.504	
		4.	1 1 −1	0.729	0.666	0.702
		4.	1 1 1		0.739	
		16.	2 2 −1	0.964	0.926	0.952
		16.	2 2 1		0.978	
		16.	2 2 0	1.399	1.395	
2 1 1 ← 2 0 2		4.	−2 −1 0	−1.903	−1.908	
		6.	−1 0 0	−1.223	−1.250	
45795.361	17.510	4.	−2 −1 −1	−1.088	−1.135	−1.086
		4.	−2 −1 1		−1.037	
		6.	−1 0 −1	−0.628	−0.670	−0.634
		6.	−1 0 1		−0.598	
		6.	1 0 −1	1.059	1.026	1.061
		6.	1 0 1		1.096	
		4.	2 1 −1	1.414	1.399	
		4.	2 1 1	1.512	1.511	
3 1 2 ← 3 0 3		36.	−3 −3 −1	−1.273	−1.289	−1.274
		36.	−3 −3 1		−1.259	
46493.486	24.895	36.	−3 −3 0	−0.985	−0.982	
		16.	−2 −2 −1	−0.735	−0.750	−0.733
		16.	−2 −2 0		−0.744	
		16.	−2 −2 1		−0.706	
		4.	−1 −1 −1	−0.251	−0.272	−0.252
		4.	−1 −1 1		−0.233	
		16.	2 2 −1	0.748	0.706	0.733
		16.	2 2 0		0.738	
		16.	2 2 1		0.754	
		36.	3 3 −1	0.889	0.884	0.896
		36.	3 3 1		0.909	
		36.	3 3 0	1.172	1.178	

Since the strong magnetic field effectively uncouples ^{14}N spin and overall rotation, the Hamiltonian matrix was set up in the uncoupled asymmetric top basis $|J, K_a K_c, M_J, I, M_I\rangle$ as described earlier [18]. Matrix elements connecting different rotational states i.e. states with different J, $K_a K_c$ quantum numbers, were neglected. From a second order treatment their contributions to the satellite frequencies may be estimated to be less than 1 kHz, which is still below the accuracy of our frequency determinations. The resulting M_J, M_I-submatrices were diagonalized numerically and the electric dipole moment transition matrix elements were subjected to the corresponding unitary transformation in order to obtain accurate satellite intensities. In Table 3 we present the results of our high field rotational Zeeman effect investigation. The satellites are designated by the M_J and M_I quantum numbers of the uncoupled wavefunctions which contribute most to the corresponding eigenfunctions.

As has been discussed earlier [19] only the absolute values and the relative sign of the g-values can be determined from such a high field study. The presence of the ^{14}N quadrupole nucleus however provides the unique opportunity to determine also the correct signs from the experiment since the quadrupole coupling introduces nonvanishing matrix elements between different M_J, M_I states. Such nonvanishing elements exist between $\langle M_J, M_I|$ and $|M_J \pm 1, M_I \mp 1\rangle$ uncoupled states and between $\langle M_J, M_I|$ and $|M_J \pm 2, M_I \mp 2\rangle$ uncoupled states and depending on the different choice of the sign of the g-value they connect differently spaced states which in turn causes different shifts of the corresponding energy levels. This is demonstrated for the 1_{01} rotational state in Figure 3. Explicit expressions for all matrix elements have been given earlier [20]. In Fig. 4 we present the 8.8 kG multiplets calculated for the two different sets of g-tensor elements which are compatible with the observed high field pattern together with the corresponding observed Zeeman hfs multiplet. From the comparison, the set of positive g-values must be discarded. In Fig. 5 we demonstrate how the high field uncoupled Zeeman-hfs-multiplet the $1_{01} \leftarrow 0_{00}$ transition develops from the zero field ^{14}N-hfs multiplet.

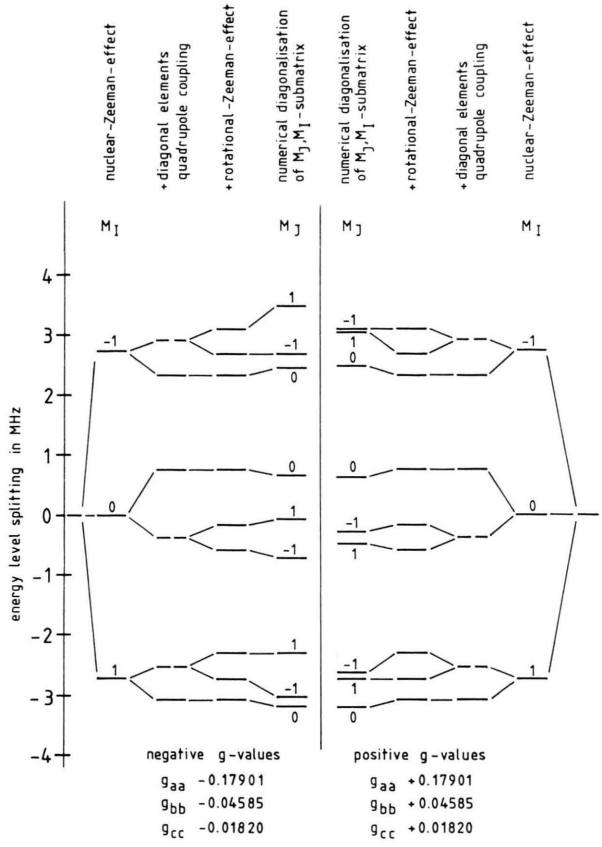

Fig. 3. Energy level scheme of the M_J, M_I-sublevels of the 1_{01} rotational state at a magnetic field of 8.8 kGauß as it develops within the uncoupled basis if the matrix elements are accounted for in a sequential manner. Within the uncoupled basis only the nuclear quadrupole coupling introduces off diagonal elements within the 1_{01}-subspace. Nonvanishing elements exist between $\langle M_J, M_I|$ and $|M_J \pm 1, M_I \mp 1\rangle$ states and $\langle M_J, M_I|$ and $|M_J \pm 2, M_I \mp 2\rangle$ states respectively. At such intermediate fields their effect on the final position of the levels is appreciable and the level schemes which arise for the two sets of g-values are clearly distinguishable.

Table 4. Diagonal elements of the molecular g-tensor and anisotropies in the diagonal elements of the molecular magnetic susceptibility tensor resulting from a least squares fit to the $\Delta\nu_{exp}$-values listed in Table 3. For this fit we have used the rotational constants and quadrupole coupling constants listed in Table 2. A second set of g-values (all signs reversed) would be also compatible with the observed high field Zeeman hfs patterns but it could be descarded on the basis of intermediate field spectra such as shown in Figure 4.

g_{aa}	−0.17901(33)	
g_{bb}	−0.04585(17)	
g_{cc}	−0.01820(16)	
$2\chi_{aa} - \chi_{bb} - \chi_{cc}$	−7.22(25)	10^{-6} erg G^{-2} mole^{-1}
$2\chi_{bb} - \chi_{cc} - \chi_{aa}$	15.90(31)	10^{-6} erg G^{-2} mole^{-1}

This computersimulation is based on the molecular parameters in Tables 2 and 4.

Finally we have used the high field Zeeman uncoupling of ^{14}N nuclear spin and overall rotation to determine improved values for the two nonvanishing vibronic ground state expectation values of the molecular electric dipole moment μ_a and μ_b. To this end a set of dc Stark effect voltages were superimposed to the modulating Stark field (electric Stark field and magnetic Zeeman field parallel). To account for the potential energy of the molecular electric dipole moment within this applied electric field, E_Z, the effective Hamiltonian (Eqs. (1) through (4)) has to be supplemented by a fifth term, $\hat{H}_{\text{Stark}}$:

$$\hat{H}_{\text{Stark}} = -\mu_a \hat{\Phi}_{aZ} E_Z - \mu_b \hat{\Phi}_{bZ} E_Z . \tag{5}$$

Within the uncoupled basis the direction cosine matrix elements $\langle \hat{\Phi}_{aZ} \rangle$ and $\langle \hat{\Phi}_{bZ} \rangle$ are diagonal in M_J (and I, M_I).

Therefore, provided the strong Zeeman field has indeed sufficiently uncoupled ^{14}N spin and overall angular momentum, the usual second order perturbation treatment for rigid rotor molecules without quadrupole nuclei can be used to a good approximation (accuracy is on the order of 1‰) to analyze the Stark effect shifts of the M_J-satellites from their zero Stark-field position [21].

In Fig. 6 we illustrate the underlying idea in a computersimulation for the $2_{11} \leftarrow 2_{02}$ rotational transition. In Table 5 we list the Stark effect shifts of those M_J-satellites which were used for the least squares fit of the dipole moment components together with the optimized dipole moment components μ_a and μ_b.

Diagonal Elements of the Molecular Electric Quadrupole Moment Tensor and other Molecular Properties

Substituting the experimental g-values, susceptibilities and principal moments of inertia into the corresponding theoretical expressions (see (2) and (3)) gives the diagonal elements of the molecular electric quadrupole moment tensor:

$$Q_{aa} = \frac{|e|}{2} \left\{ \sum_{\nu}^{\text{nuclei}} Z_\nu (2a_\nu^2 - b_\nu^2 - c_\nu^2) - \langle 0 | \sum_{\varepsilon}^{\text{electrons}} 2a_\varepsilon^2 - b_\varepsilon^2 - c_\varepsilon^2 | 0 \rangle \right\}$$

$$= -\frac{|e|}{2m_p} (2I_{aa}g_{aa} - I_{bb}g_{bb} - I_{cc}g_{cc}) - \frac{2mc^2}{|e|} (2\chi_{aa} - \chi_{bb} - \chi_{cc}) \tag{6}$$

(and cyclic permutations).

They are referred to the principal inertia axes system (see Figure 1). From Costains structure and the experimental g-values and rotational constants we are also in the position to give the so called paramagnetic susceptibilities.

$$\chi_{aa}^{(p)} = -\frac{e^2}{2m^2c^2} \left(\frac{L_a L_a}{\Delta} \right) = -\frac{e^2}{4mc^2} \left(\frac{I_{aa}g_{aa}}{m_p} - \sum_{\nu}^{\text{nuclei}} Z_\nu (b_\nu^2 + c_\nu^2) \right) \tag{7}$$

(and cyclic permutations).

They are closely related to the electron contribution to the molecular moments of inertia [22, 23].

Also the anisotropies of the second moments of the electronic charge distribution are directly obtained from our data:

$$\langle 0 | \sum_{\varepsilon}^{\text{electrons}} (a_\varepsilon^2 - b_\varepsilon^2) | 0 \rangle = \sum_{\nu}^{\text{nuclei}} Z_\nu (a_\nu^2 - b_\nu^2) + \frac{1}{m_p} (I_{aa}g_{aa} - I_{bb}g_{bb}) + \frac{4mc^2}{3e^2} \{ (2\chi_{aa} - \chi_{bb} - \chi_{cc}) - (2\chi_{bb} - \chi_{cc} - \chi_{aa}) \} . \tag{8}$$

Just as the molecular electric quadrupole moments, they are of interest to probe the accuracy of ab initio wavefunctions in the outer regions of the molecule.

If the bulk susceptibility is known, it is also possible to determine the diagonal elements of the magnetic susceptibility tensor. To our knowledge no accurate value for the bulk susceptibility of Acrylonitrile has been measured so far. We therefore used the system developed by Haberditzl [24] to calculate the bulk susceptibility from inner shell (atom) increments and bond increments. The so calculated bulk susceptibility typically agrees within 1% with the experimental value [25]. For error propagation we therefore assume a conservative ±4% uncertainty in the calculated bulk value. The calculation of the bulk value is given in Table 6.

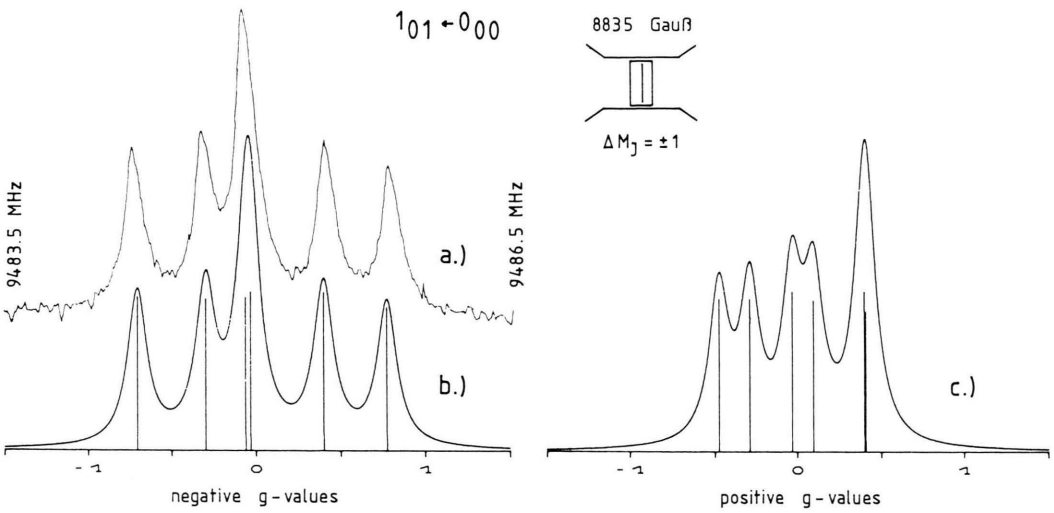

Fig. 4. Zeeman-hfs-multiplets of the $1_{01} \leftarrow 0_{00}$ transition of Acrylonitrile at a field of 8835 Gauß: a) experimental spectrum, b) simulation using the data of Table 4 and g-values with negative sign, c) simulation from g-values with positive sign. From the comparison of the line shapes it is obvious that the set with positive g-values must be discarded.

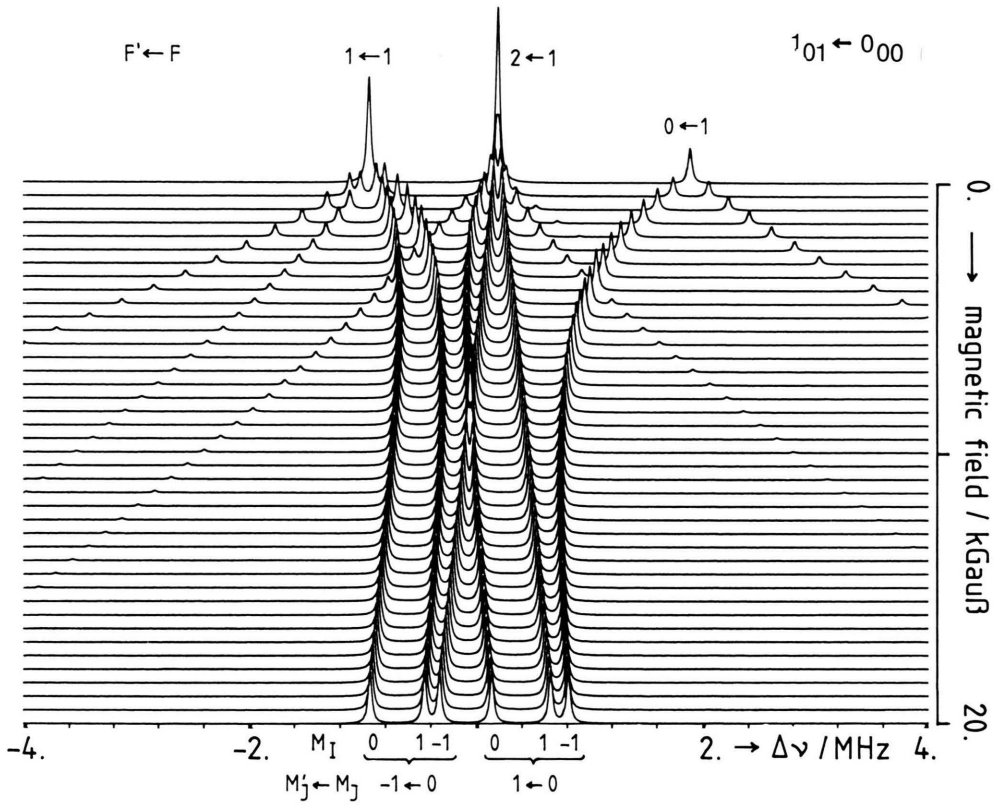

Fig. 5. Simulation demonstrating how the Zeeman-hfs-multiplet develops from the zero field hfs multiplet (uppermost trace, compare Figure 2). The zero field hfs-satellites are designated by the F-quantum numbers ($\boldsymbol{F} = \boldsymbol{J} + \boldsymbol{I}$ (^{14}N)) of the lower and the upper rotational states. From trace to trace the magnetic field increases in steps of 500 Gauß. At low fields (below 2 kGauß) the coupled basis $|J, K_a K_c, I, F, M_F\rangle$ with the electric dipole selection rule $\Delta M_F = \pm 1$ is appropriate to describe the splittings. At high fields, where the ^{14}N nuclear Zeeman effect uncouples spin and overall rotation, the uncoupled basis $|J, K_a K_c, M_J, I, M_I\rangle$ is appropriate and the selection rules $\Delta M_J = \pm 1$ and $\Delta M_I = 0$ apply. The satellites are designated accordingly. The simulation is based on the molecular constants given in Tables 2 and 4 (negative g-values).

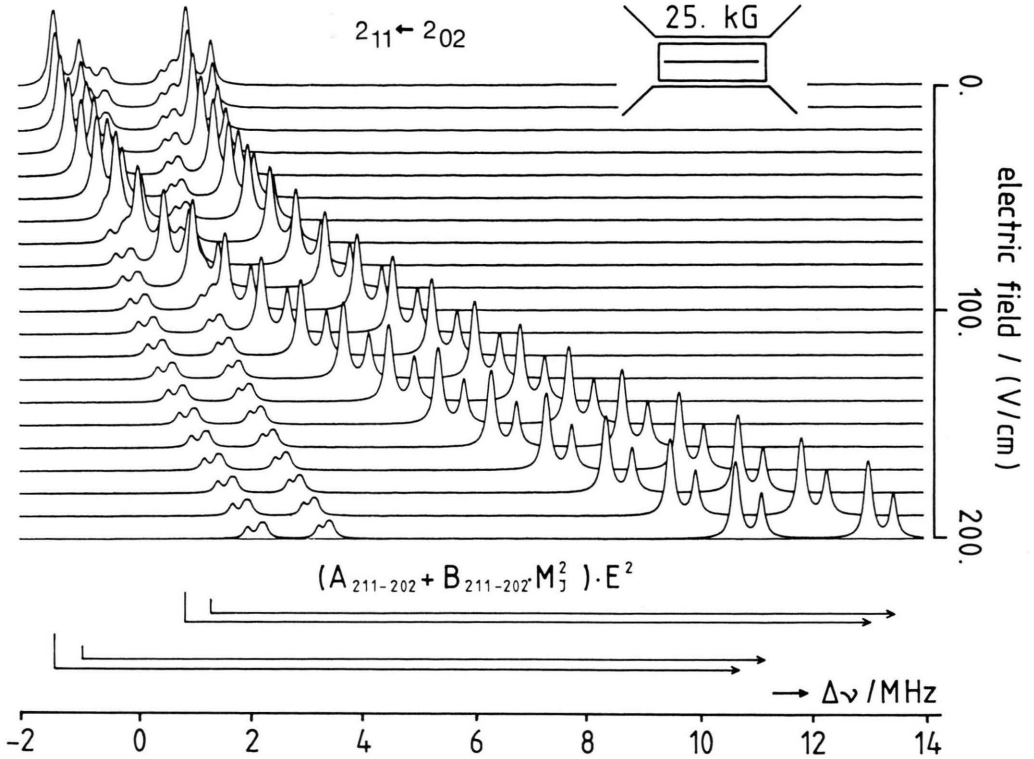

Fig. 6. Computersimulation of the Zeeman-hfs-Stark-patterns of the $2_{11} \leftarrow 2_{02}$ rotational transition at a magnetic field of 25 kGauß. The field effectively uncouples ^{14}N spin and overall rotation. With magnetic field, Stark field and electric field of the incident microwave field all parallel, $\Delta M_J = 0$, $\Delta M_I = 0$ selection rules apply. The Stark field increases from zero (uppermost trace) to 200 V/cm (lowest trace) in steps of 10 V/cm. From second order perturbation theory the Stark shifts of the satellites from their zero Stark field positions obey the $(A + B \cdot M^2) \cdot E_Z^2$ law where A and B depend on the components of the electric dipole moments just as in the case of the rigid rotor (Ref. [17], Chapt. 10.3 a). Lorentzian line shapes with 140 kHz full width at half height are used in this simulation. Additional line broadening due to the inhomogeneity of the Stark field is not accounted for. Also the slight additional broadening due to the crossfield Lorentz-Stark-effect (Ref. [9], p. 137–142) has been neglected in this simulation.

Table 5. Experimental and calculated Stark-effect-shifts, used to fit the dipole moment components μ_a and μ_b of Acrylonitrile. With average Stark-effect-shifts (column 4) we mean the average value from the observed shifts of corresponding M_J-satellites with respect to their zero Stark-field positions (compare Figure 6). There are 4 such satellites with quantum numbers $M_I = 0$ and $M_I = \pm 1$, for each M_J value. (The $M_I = +1$ and $M_I = -1$ satellites are not resolved and merge to one line with twice the intensity of the corresponding $M_I = 0$ satellite). The uncertainties of the dipole moment components are single standard uncertainties and include a 0.25% calibration uncertainty.

Transition $J'\ K_a'\ K_c' \leftarrow J\ K_a\ K_c$	$\lvert M_J \rvert$	E_Z/(V/cm)	exp. average Stark-effect-shift MHz	calc. Stark-effect-shift MHz
2 1 1 ← 2 0 2	2	21.2	0.129	0.135
	2	42.3	0.528	0.541
	2	84.6	2.171	2.162
3 1 2 ← 3 0 3	2	63.5	0.133	0.154
	2	105.8	0.415	0.429
	2	148.1	0.837	0.840
	2	253.9	2.480	2.470
	3	63.5	0.343	0.352
	3	105.8	0.975	0.978
	3	148.1	1.911	1.917

$\lvert \mu_a \rvert = 3.815(12)$ D
$\lvert \mu_b \rvert = 0.894(68)$ D
$\lvert \mu_{tot} \rvert = 3.918(69)$ D

Table 6. Calculation of the bulk susceptibility of Acrylonitrile within the Haberditzl scheme [24]. At the Carbon atoms the lower indices (here 1 or 2) indicate the number of Hydrogens which are replaced by a more electronegative substituent. An upper "+" at C indicates a sp^2 hybridized Carbon atom, an upper "0" indicates a sp-hybridized Carbon atom. For the $C_2^+ - C_1^0$ bond, for which no increment is given in [24], we have used the $C^+ - C^+$ increment. All values are in units of 10^{-6} erg G^{-2} $mole^{-1}$.

	Core or bond	Contribution to χ_{bulk}
cores	3 ©	−0.45
	1 Ⓝ	−2.4
bonds	2 $C_1^+ - H$	−7.2
	1 $C_2^+ - H$	−3.2
	2 $C^+ - C^+$	−4.8
	1 $C_1^+ \pi C_2^+$	−3.4
	1 $C^0 \equiv N$	−9.2

Table 7. Molecular quantities, derived from the data of Table 4, the geometry of the nuclear frame and the bulk magnetic susceptibility which was calculated within the Haberditzl scheme as described in the text.

$\chi = (\chi_{aa} + \chi_{bb} + \chi_{cc})/3$	−30.7(12)	10^{-6} erg G^{-2} $mole^{-1}$
Q_{aa}	−3.23(24)	10^{-26} esu cm^2
Q_{bb}	4.04(31)	10^{-26} esu cm^2
Q_{cc}	−0.81(45)	10^{-26} esu cm^2
χ_{aa}	−33.1(13)	10^{-6} erg G^{-2} $mole^{-1}$
χ_{bb}	−25.4(13)	10^{-6} erg G^{-2} $mole^{-1}$
χ_{cc}	−33.6(14)	10^{-6} erg G^{-2} $mole^{-1}$
$\chi_{aa}^{(p)}$	38.7(1)	10^{-6} erg G^{-2} $mole^{-1}$
$\chi_{bb}^{(p)}$	257.1(2)	10^{-6} erg G^{-2} $mole^{-1}$
$\chi_{cc}^{(p)}$	277.1(2)	10^{-6} erg G^{-2} $mole^{-1}$
$\sum_{\nu}^{\text{nuclei}} Z_\nu a_\nu^2$	55.96(1)	Å^2
$\sum_{\nu} Z_\nu b_\nu^2$	7.32(1)	Å^2
$\sum_{\nu} Z_\nu c_\nu^2$	0.00	Å^2
$\langle 0 \vert \sum_{\varepsilon}^{\text{electrons}} (a_\varepsilon^2 - b_\varepsilon^2) \vert 0 \rangle$	49.65(8)	Å^2
$\langle 0 \vert \sum_{\varepsilon} (b_\varepsilon^2 - c_\varepsilon^2) \vert 0 \rangle$	6.64(12)	Å^2
$\langle 0 \vert \sum_{\varepsilon} (c_\varepsilon^2 - a_\varepsilon^2) \vert 0 \rangle$	−56.29(10)	Å^2
$\langle 0 \vert \sum_{\varepsilon} a_\varepsilon^2 \vert 0 \rangle$	61.43(52)	Å^2
$\langle 0 \vert \sum_{\varepsilon} b_\varepsilon^2 \vert 0 \rangle$	11.78(52)	Å^2
$\langle 0 \vert \sum_{\varepsilon} c_\varepsilon^2 \vert 0 \rangle$	5.14(52)	Å^2

Within this approach the calculated value is

$$\chi = (\chi_{aa} + \chi_{bb} + \chi_{cc})/3 = (-30.7 \pm 1.2)\ 10^{-6}\ \text{erg}\ G^{-2}\ \text{mol}^{-1}.$$

We note that this value essentially agrees with a value calculated from the experimental bulk susceptibility of Ethylene $\chi(\text{H}_2\text{C}{=}\text{CH}_2) = -19.0 \cdot 10^{-6}$ erg G^{-2} $mole^{-1}$ [26] and an average increment of $(-10.3 \pm 0.7) \cdot 10^{-6}$ erg G^{-2} $mole^{-1}$ for the replacement of a Hydrogen atom by a Nitrile group [27].

In Table 7 we present the molecular electric quadrupole moments and the other vibronic ground state properties which may be derived from the Zeeman data, the r_s-structure and the extrapolated value for the bulk susceptibility.

Discussion

In the discussion we will focus our interest on two aspects of our results: on the observed ^{14}N nuclear quadrupole coupling constants and on the magnetic susceptibilities.

Only the diagonal elements of the quadrupole coupling tensor referred to the principal inertia axes are determined from the experiment. The off-diagonal element, χ_{ab}^N, whose value should be close to −0.56 MHz (see below), contributes only in second order to the observed hfs-splittings, and this is below the experimental accuracy of the present investigation.

In a certain sense we may however overcome this lack of experimental information by making an assumption. In the first run we assume that the C−C≡N chain is indeed linear as suggested by Costains data and that the principal axes system of the coupling tensor is aligned to the N≡C-internuclear axis (x-axis = bond axis, y-axis in the plane of the nuclei, z-axis parallel to the molecular c-axis i.e. out of plane axis). With these assumptions we may use the measured values for χ_{aa} and χ_{bb} to calculate the coupling tensor elements in its principal axes system from

$$\begin{aligned}\chi_{aa}^N &= \cos^2(a\,x)\,\chi_{xx}^N + \cos^2(a\,y)\,\chi_{yy}^N \\ &= \cos^2\alpha\,\chi_{xx}^N + \sin^2\alpha\,\chi_{yy}^N, \\ \chi_{bb}^N &= \cos^2(b\,x)\,\chi_{xx}^N + \cos^2(b\,y)\,\chi_{yy}^N \\ &= \sin^2\alpha\,\chi_{xx}^N + \cos^2\alpha\,\chi_{yy}^N. \end{aligned} \tag{9}$$

With $\alpha = 15.98°$ from Costains work (see Fig. 1) we obtain:

$\chi^N_{xx} = -4.2677(23)$ MHz, $\chi^N_{yy} = 2.1677(50)$ MHz,
$\chi^N_{zz} = 2.1000(46)$ MHz $= \chi^N_{cc}$.

These values should be compared to the corresponding experimental values determined for Benzonitrile [28]:

$\chi^N_{xx} = -4.187(70)$ MHz, $\chi^N_{yy} = +2.301(80)$ MHz,
$\chi^N_{zz} = +1.886(80)$ MHz.

Within a simplified MO-treatment [29] they may be used to estimate the population difference in the out of plane and in plane Nitrogen p-orbitals perpendicular to the C≡N bond as

$$P_{p_z p_z} - P_{p_y p_y} = 2 \sum_{n}^{\text{occupied orbitals}} (C^2_{np_z}(^{14}\text{N}) - C^2_{np_y}(^{14}\text{N}))$$

$$= \frac{2}{3eQq_{2,1,0}} (\chi^N_{zz} - \chi^N_{yy}) . \qquad (10)$$

Here $C_{np_z}(^{14}\text{N})$ is the LCAO-coefficient for the p_z-orbital at the Nitrogen in the n-th occupied molecular orbital etc.

With $eQq_{2,1,0} = -10$ MHz [30], the population difference if calculated according to (10), turns out to be positive in both cases, i.e. the more electronegative Nitrogen atom has pulled electron density more readily from the p_z-orbitals of the attached π-system than from the in plane orbitals. In organic chemistry this pulling is called the mesomeric effect of the −C≡N group. We must note, however, that the approximations which lead to (10) correspond to an uncertainty on the order of at least 200 kHz in the interpretation of the coupling constants. (This is a typical value for D-quadrupole coupling constants, which should be zero within the above approximation.)

From the above values for χ^N_{xx} and χ^N_{yy} we may also estimate the value of χ^N_{ab} as (compare Fig. 1):

$$\chi^N_{ab} = \cos(ax)\cos(bx)\chi^N_{xx} + \cos(ay)\cos(by)\chi^N_{yy} = -0.556 \text{ MHz} .$$

This value makes it possible to check numerically whether or not the neglect of χ^N_{ab} in the analysis of the hyperfine splittings was justified. It was.

In a second run we might make a different assumption and follow the argument of Cox et al. [31] who assume that quite in general the quadrupole coupling tensor of ^{14}N if attached to a non aromatic frame, has cylindrical symmetry about the −C≡N bond axis i.e.

$$\chi^N_{yy} = \chi^N_{zz} = \chi^N_{cc} \quad \text{and}$$
$$\chi^N_{xx} = -(\chi^N_{yy} + \chi^N_{zz}) = -2\chi^N_{cc} .$$

Eq. 9 may than be used to calculate the angle α as 14.97° i.e. the C≡N bond axis would be titled towards the a-axis by 1°. This decreased angle together with the well determined r_s-difference in the a-coordinates of the Nitrogen and the adjacent carbon atom from Costains work [2], $a_C - a_N = 1.1187$ Å, leads to the possibility to redetermine the CN internuclear distance as

$$r_{C\equiv N} = (a_C - a_N)/\cos(14.97°) = 1.158 \text{ Å} .$$

This result is in excellent agreement with the observation of Cox et al., that the r_s bond distance in Nitriles "shows a remarkably constant value close to 1.158 Å".

For a final discussion the direct and accurate determination of χ^N_{ab} would be necessary which, at present, is still beyond the resolution power of our spectrometers.

We now turn to the discussion of the magnetic susceptibilities and to the local susceptibility tensor of the C≡N group.

In 1973 Schmalz, Norris, and Flygare [32] have proposed a simple additivity scheme to calculate the susceptibility tensor of open chain molecules from local (atom-)tensors. An extended list of local susceptibilities based on the work of Wiese [33] together with detailed description of the procedure has been given in [9], p. 104–114.

Even though the additivity scheme works well in many cases, there are now some examples which indicate that the scheme needs refinement [34].

At present we feel that the appropriate building blocks should be choosen larger than originally assumed and we think that the concept of localized molecular orbitals provides a reasonable guide line to the size of the subunits to be used in the scheme. To illustrate the idea we consider the two occupied canonical π-orbitals in Acrylonitrile as they are calculated with the semiempirical CNDO/2 programm [35]. We will designate them as ψ_1 and ψ_2.

Their LCAO-coefficients for the carbon and nitrogen p_z-orbitals are given in Figure 7. Since every unitary transformation among the occupied molecular orbitals leaves the corresponding Slater determinant i.e. the electronic ground state wave-

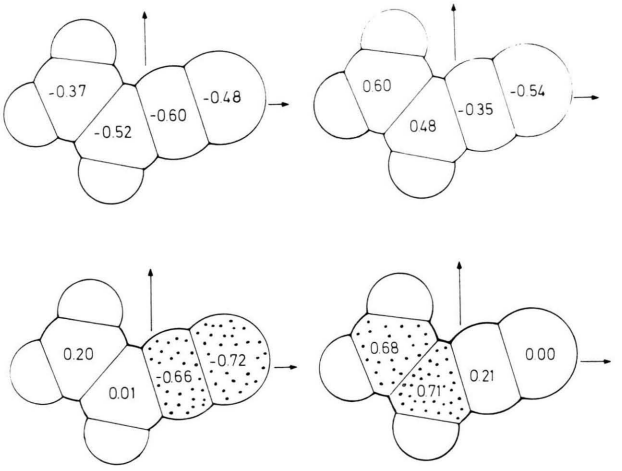

Fig. 7. LCAO coefficients for the p_z-orbitals of the two occupied π-orbitals of Acrylonitrile as calculated within the CNDO/2 approximation are shown in the upper part of this Figure. In the lower part we give the corresponding coefficients for the localized π-orbitals. Orbital density is concentrated in the region of the C≡N group (left) or in the region of the C=C group (right). The coefficients shown here follow from the criterium that the π-density at the Nitrogen should be extremized. The same overall picture is obtained however if any one of the C-atoms is choosen as center of localization. The Figure indicates that the C≡N group as a whole should be used as a subunit, if one breaks down the molecular magnetic susceptibility tensor into local increments.

function invariant, we may try a new set of molecular orbitals defined by $\psi_+ = \cos(\varphi)\,\psi_1 + \sin(\varphi)\,\psi_2$ and $\psi_- = -\sin(\varphi)\,\psi_1 + \cos(\varphi)\,\psi_2$ to replace the original canonical orbitals ψ_1 and ψ_2 in the Slater determinant without changing the overall electronic wavefunction.

We might now choose φ such that the Coulomb self energy of the orbital ψ_+ is maximized [36], i.e. that

$$\int\int \frac{|\psi_+(\boldsymbol{r}_1)|^2 \cdot |\psi_+(\boldsymbol{r}_2)|^2}{|\boldsymbol{r}_1 - \boldsymbol{r}_2|}\, d\tau_1\, d\tau_2 \Rightarrow \text{maximum}\,.$$

For the purpose of the present more qualitative discussion it may however be sufficient to require that for instance the LCAO coefficient for the Nitrogen p_z-orbital should be maximized. (Only one condition can be imposed in our case of two molecular orbitals. The second orbital follows automatically from the orthonormality condition.) With the above choice the value for φ is determined by

$$C_+(N) = \cos(\varphi)\,C_1(N) + \sin(\varphi)\,C_2(N) \stackrel{!}{=} \text{Max}$$

Table 8. Local susceptibility tensors for Hydrogen and the $\diagdown C{=}C \diagup$ group taken from Table II.2 of [9]. Also given is the susceptibility tensor for the Nitrile group derived from χ_{aa}, χ_{bb} and χ_{cc} of Acrylonitrile and the local increments for H− and $\diagdown C{=}C \diagup$ determined earlier (see Table II.2 of [9]). Cylindrical symmetry of the C≡N group is assumed. All values are given in units of 10^{-6} erg G^{-2} mole^{-1}.

$\overset{y}{\underset{x}{\hookrightarrow}}$	χ_{xx}	χ_{yy}	χ_{zz}
H−	−1.17(53)	−2.08(38)	−2.08(38)
$\diagdown C{=}C \diagup$	−7.28(72)	−7.50(85)	−14.66(78)
−C≡N	−21.0(19)	−12.85(210)	−12.85(210)

which is equivalent to

$$\sin(\varphi)/\cos(\varphi) = C_2(N)/C_1(N) = 0.54/0.48\,,$$

or $\varphi = 48.37°$.

The result is depicted on the lower half of Figure 7. As is clearly seen, each "localized" molecular π-orbital still stretches over two atoms, the C=C group or the C≡N group. We note that this general result is independent of the special choise for the LCAO-coefficient to be maximized. If one chooses instead the coefficient of one of the carbon p_z-orbitals, the same overall picture is obtained with only minor changes in the LCAO-coefficients for the localized molecular orbitals. As a consequence we think that the most appropriate choice to break down the molecular susceptibility tensor of Acrylonitrile is to use the three Hydrogens, H−, the C=C group, and the C≡N group as subunits. Then from the geometry (see Fig. 1) and from the local susceptibility tensors for H− and C=C from the work of Wiese [33], we may derive components for the yet unknown susceptibility tensor of the C≡N group from the equations:

$$\chi_{aa} = \sum_i^{\text{subunits}} (\cos^2(a\,x_i)\,\chi_{xx,i} + \cos^2(a\,y_i)\,\chi_{yy,i})\,,$$

$$\chi_{bb} = \sum_i^{\text{subunits}} (\cos^2(b\,x_i)\,\chi_{xx,i} + \cos^2(b\,y_i)\,\chi_{yy,i})\,,$$

$$\chi_{cc} = \sum_i^{\text{subunits}} \chi_{zz,i}\,, \qquad (11)$$

where the index i runs over the three Hydrogens, the C=C group and the C≡N group. The orientation of the χ-tensors and the tensorelements for the subunits are given in the upper part of Table 8. The

angles follow from Figure 1. The left hand sides follow from the measured susceptibility anisotropies and the calculated bulk susceptibility (see Table 4). Solving for the elements for the susceptibility tensor of the Nitrile group leads to

χ_{xx}, (C≡N) = (−21.0 ± 1.9) 10^{-6} erg G^{-2} $mole^{-1}$,

χ_{yy}, (C≡N) = (−13.0 ± 2.1) 10^{-6} erg G^{-2} $mole^{-1}$,

χ_{zz}, (C≡N) = (−12.7 ± 2.0) 10^{-6} erg G^{-2} $mole^{-1}$

(x-axis along the C≡N-bond, z-axis perpendicular to the molecular plane).

The uncertainties are single standard uncertainties. They follow by standard error propagation from the quoted uncertainties in the Hydrogen and sp^2-Carbon contributions (see Table 5), from the experimental uncertainties in the susceptibility anisotropies (see Table 4) and from the 4% uncertainty which was assumed for the calculated molecular bulk susceptibility.

We note the close agreement between the two independently determined components perpendicular to the bond axis. The CN group indeed shows the expected cylindrical symmetry also from the point of view of its magnetic properties. We further note that with χ(C≡N) = (−15.6 ± 1.2) 10^{-6} erg G^{-2} $mole^{-1}$ the average trace for the CN-tensor contribution is within two standard deviations from the value of (−13.1 ± 0.51) 10^{-6} erg G^{-2} $mole^{-1}$ which would be expected from the Haberditzl-scheme (4% uncertainty assumed).

We therefore believe that the susceptibility tensor for the Nitrile group determined here is already sufficiently accurate to be of use for the calculation of shielding contributions of Nitrile groups in NMR-spectra.

Acknowledgement

We would like to thank Prof. H. Dreizler for critically reading the manuscript. The financial support from the Deutsche Forschungsgemeinschaft and Fonds der Chemie is also gratefully acknowledged. All computer calculations were performed at the PDP 10 Computer of the Computer Center at the University of Kiel.

[1] W. S. Wilcox, J. H. Goldstein, and S. W. Simmons, J. Chem. Phys. **22,** 516 (1954).
[2] C. C. Costain and B. P. Stoicheff, J. Chem. Phys. **30,** 777 (1959).
[3] Values are recalculated from the hfs patterns, published in [2] since incomplete information on the experimental uncertainties had been given by the authors.
[4] J. Demaison, A. Bouchy, G. Roussy, and J. Barriol, C. R. Acad. Sci. Paris **276 C,** 967 (1973).
[5] M. C. L. Gerry and G. Winnewisser, J. Mol. Spectry **48,** 1 (1973).
[6] F. F. Gardner and G. Winnewisser, Astrophys. J. **195,** L 127 (1975).
[7] M. C. L. Gerry, K. Yamada, and G. Winnewisser, J. Phys. Chem. Ref. Data **8,** 107 (1979).
[8] D. H. Sutter, Z. Naturforsch. **26 a,** 1644 (1971).
[9] D. H. Sutter and W. H. Flygare, Topics in Current Chemistry **63,** 115 (1976).
[10] W. H. Stolze, M. Stolze, D. Hübner, and D. H. Sutter, Z. Naturforsch. **37 a,** 1165 (1982).
[11] M. Stolze, D. Hübner, and D. H. Sutter, J. Molec. Struct. **97,** 243 (1983).
[12] H. D. Rudolph, Z. Naturforsch. **23 a,** 540 (1968).
[13] Ref. [9], p. 121–147.
[14] H. B. Benz, A. Bauder, and Hs. H. Günthard, J. Mol. Spectr. **21,** 156 (1966).
[15] M. Stolze, D. Hübner, and D. H. Sutter, Z. Naturforsch. **36 a,** 886 (1981).
[16] Ref. [9], p. 139, 144.
[17] W. Gordy and R. L. Cook, Microwave Molecular Spectra, Interscience Publishers, New York 1970, p. 654.
[18] E. Hamer, Dissertation, Kiel 1973.
[19] Ref. [9], p. 145.
[20] Ref. [9], p. 131, 144, 145.
[21] W. Czieslik, Diplomthesis, Kiel 1972, p. 19–24.
[22] C. H. Townes and A. L. Schawlow, Microwave Spectroscopy, Dover Publications, Inc. New York 1975, p. 212–215.
[23] Ref. [9], p. 173.
[24] W. Haberditzl, Sitzungsberichte der Deutschen Akademie der Wissenschaften zu Berlin, Klasse für Chemie, Geologie und Biologie, Jahrgang 1964, Nr. 2.
[25] Ref. [24], p. 39.
[26] Ref. [24], p. 48.
[27] W. H. Stolze and D. H. Sutter, Z. Naturforsch. **39 a,** 1092 (1984).
[28] E. Fliege, G. Bestmann, R. Schwarz, and H. Dreizler, Z. Naturforsch. **36 a,** 1124 (1981).
[29] J. Mjöberg and S. Ljunggren, Z. Naturforsch. **28 a,** 729 (1973).
[30] Ref. [17], Chapt. 14.13.
[31] A. P. Cox and Y. Kawashima, E. Fliege, and H. Dreizler, Z. Naturforsch. **40 a,** 361 (1985).
[32] R. G. Schmalz, C. C. Norris, and W. H. Flygare, J. Amer. Chem. Soc. **94,** 796 (1973).
[33] J. Wiese, Diplomthesis, Kiel 1975.
[34] D. Hübner and D. H. Sutter, Z. Naturforsch. **39 a,** 55 (1984).
[35] J. A. Pople and D. L. Beveridge, Approximate Molecular Orbital Theory, McGraw-Hill, New York 1970.
[36] W. England, L. S. Salmon, and K. Ruedenberg, Topics Current Chem. **23,** 31 (1971).